AN ADAPTIVE MORPHOLOGICAL FILTER FOR DEFECT DETECTION IN EDDY CURRENT AIRCRAFT WHEEL INSPECTION

Shu Gao, Lalita Udpa
Department of Electrical Engineering and Computer Engineering
Iowa State University
Ames, IA 50010

INTRODUCTION

Eddy current technique is a widely used nondestructive testing (NDT) method in aircraft wheel inspection. Commercial wheel inspection systems used by airlines perform a helical scan of the wheel outer surface and produce a strip chart record of the inspection signal. In practice, the eddy current signals are often contaminated by noise, which makes the interpretation of the strip chart record very difficult. In commercial systems, the problem of data interpretation is rendered difficult due to the fact that the hardware configuration (narrow band pre-filter and low sampling rate) eliminates the information about the shape and spectral differences between the defect signal and noise. In order to improve the performance of the wheel inspection system, a PC based signal analysis system was developed to obtain a more accurate interpretation of the eddy current inspection signal.

The signal analysis system displays the eddy current signal in the form of a c-scan image, with each row corresponding to one revolution of the helical scan. The eddy current image provides more information about the spatial correlation of the signal, which makes the signal interpretation easier. Although the image display greatly simplifies the signal interpretation, further image processing is still needed for accurate defect detection due to the high noise level.

The algorithm proposed in this paper uses an adaptive morphological filter. Mathematical morphology provides a nonlinear approach in signal and image processing which is based on set theory [1]. Morphological operations are composed of two elementary operations, namely, dilation and erosion. In the case of multilevel signals, dilation is defined as [2]

Dilation:
$$(f \oplus B)(x) = \max_{t}\{f(x-t) \mid t \in B\} \qquad (1)$$

Review of Progress in Quantitative Nondestructive Evaluation, Vol. 17
Edited by D.O. Thompson and D.E. Chimenti,, Plenum Press, New York, 1998

where f is the input signal and the set B is the structural element. Similarly, erosion, the dual operation of dilation, is defined as

Erosion: $$(f \ominus B)(x) = \min_{t} \{ f(x+t) \mid t \in B \} \quad (2)$$

In practice, the Equations (1) and (2) are normally implemented as the maximum or minimum value over a moving window. Two other basic operations, opening and closing, are defined in terms of dilation and erosion as follows:

Opening: $$A \circ B = (A \ominus B) \oplus B \quad (3)$$

Closing: $$A \bullet B = (A \oplus B) \ominus B \quad (4)$$

The next section explains in detail, the development of the morphological filter. The critical parameters of the of the filtering algorithm and methods for adaptation of the parameters are described in section 3. The results of implementing the approach along with discussions of the results are finally presented.

OVERALL SCHEME OF THE PROPOSED MORPOHLOGICAL FILTER

In practice, defect detection based on the strip chart data is performed according to a simple check rule. If a significant peak repeats at least twice on the strip chart record, and the spacing between the repetitions is equal to the length of one revolution, then the peaks are considered as defect signal. All isolated peaks are considered as speckle noise.

The signal analysis algorithm proposed in this paper implements the check rule in a more systematic and reliable manner. Figure 1 shows the overall approach used in the morphological filter. The algorithm is based on the detection of features in the residual image, which is the difference between the original image and a filtered version obtained by applying an 1-D morphological filter to each row of the image. A second 1-D morphological filter is then applied to each column to examine the spatial correlation of the features detected. According to the check rule, any isolated features less than 2 pixel long are removed by the second morphological filter. All structural elements used are one dimensional sets containing connected points around the center point.

As shown in Figure 1, the proposed algorithm has two branches with dual operations in each branch. The left branch operates on the positive part of the signal and the right branch operates on the negative part. For simplicity, only the left branch is discussed in the rest of this paper. The first 3 blocks, closing, opening, and dilation are 1-D morphological operations applied to each row of the image. The operations of the first block, the closing block, can be expressed by the following equations:

$$A = I \bullet S_1 = (I \oplus S) \ominus S \quad (5)$$

where I is the input image, A is the output image of the closing block, S_1 is the structural element. Let $J = I \oplus S$, Equation 5 can be expanded as

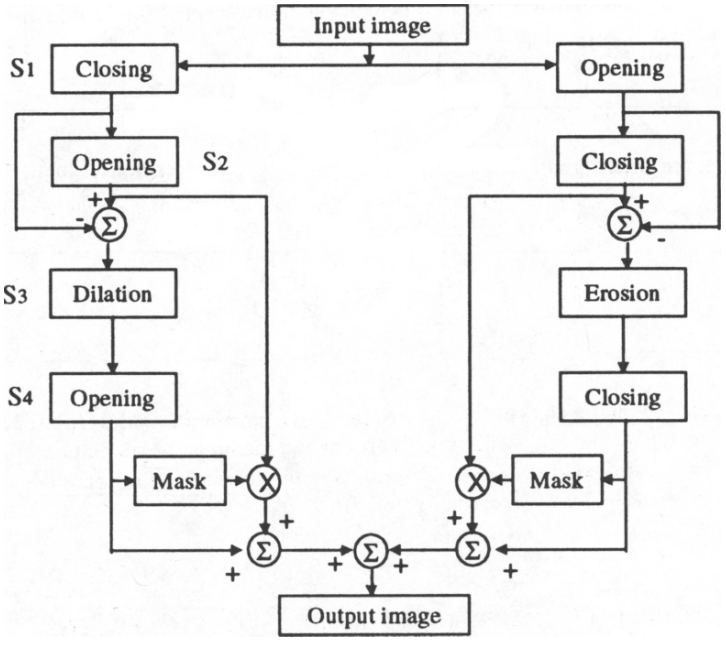

Figure 1. Overall scheme of the morphological filter.

$$J(x,y) = \max_{k}\left\{I(x,y-k)\,\middle|\,-\left\lfloor\frac{l_1}{2}\right\rfloor \le k \le \left\lfloor\frac{l_1}{2}\right\rfloor\right\} \tag{6}$$

$$A(x,y) = \min_{k}\left\{J(x,y+k)\,\middle|\,-\left\lfloor\frac{l_1}{2}\right\rfloor \le k \le \left\lfloor\frac{l_1}{2}\right\rfloor\right\} \tag{7}$$

where x and y are the row and column indices of the image, l_1 is the length of S_1. The goal of this step is to obtain the envelop of the signal. Intuitively, the closing operation fills the "valleys" between peaks of the noise while the defect spikes will remain unchanged [3]. Figure 2 (a) shows a sample signal containing a defect. The corresponding envelop signal after the closing filter is shown in Figure 2 (b). In the successive opening step, the background of the envelop signal is extracted. Here the structural element S_2 is chosen slightly larger than the size of the defect signal. The residual signal is then obtained by subtracting the background from the envelop signal. After this step, only spikes due to defects remain in the residual image and the noise is totally removed. The background of the envelop and residual signal are shown in Figures 2 (c) and (d) respectively. The dilation block operates on the residual image. In this step, each peak in the residual image is widened in the horizontal direction by the size of the structural element S_3. This step is required for detecting defects that are not vertically oriented. In this case, peaks from the

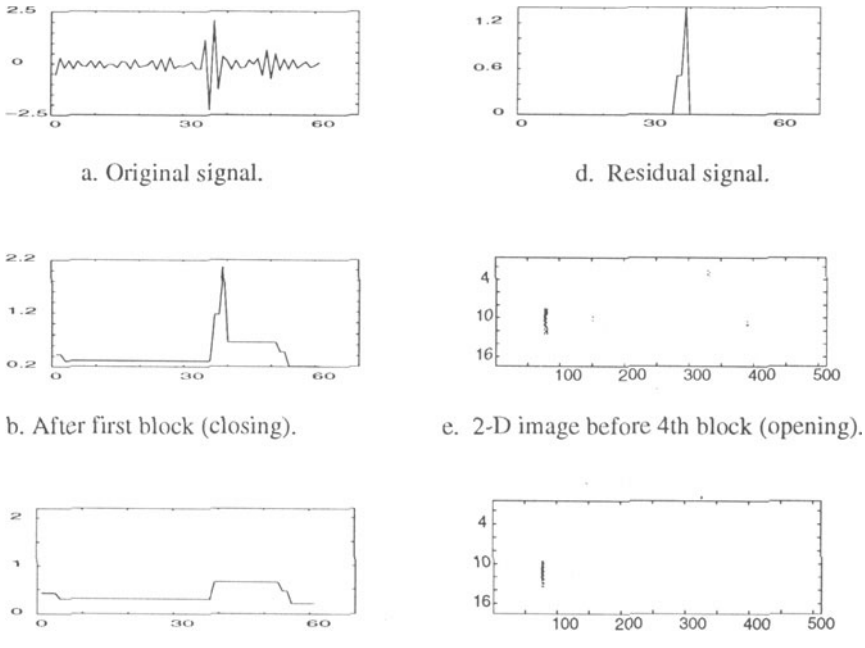

Figure 2. A sample signal at each step of the proposed morphological filter algorithm.

same defect may not be aligned in the same column of the c-scan image. The goal of this step is to therefore compensate for this situation.

The last block, the second opening block, operates on each column of the image. The purpose of this step is to examine the spatial correlation of the spikes. Any feature that is less than 2 pixel long in vertical direction is considered to be noise and is removed in this step. Figures 2 (e) and (f) show the images before and after implementing this step.

So far the defect signal has been detected and separated from the background noise. The last step of the algorithm is the "mask" operation performed to recover the actual magnitude of the defect signal and is expressed as follows:

$$P = R + B \otimes T_s(R./B) \tag{8}$$

where P is the output image of left branch, R is the residual image, and B is the back ground of the envelop signal. The symbol $\otimes$ denotes pointwise multiplication, "$./$" denotes the pointwise division and $T_s()$ is the thresholding operation

$$T_s(x) = \begin{cases} 1, & x \geq s \\ 0, & x < s \end{cases} \tag{9}$$

This thresholding eliminates features that are too small. The output images of the two branches are finally combined together by addition.

ADAPTATION OF THE FILTER

There are three structuring elements in the proposed morphological filter. The choice of the size of these structuring elements is critical to the performance of the filter. The function of the structuring element S_1 in step 1 is to obtain the envelop of the signal. The effect of this step is to fill in the "valleys" between the peaks due to noise while the defect indications remain unchanged. Therefore S_1 should be large enough to fill the "valleys" due to noise. However, when S_1 is too large, the "valley" between two adjacent defect indications will also be filled, resulting in a miss. Therefore the size of S_1 has to be selected with care so as to maximize the probability of detection (POD) and minimize the probability of false alarm (PFA).

The best way to optimize the choice of S_1 is to set the size adaptively [4]. In the noise region, the size should be large enough to avoid any false alarm, while near the defect signal, the size should be small enough to maintain the detection rate. In this study the second order moment of the local signal histogram is used to adapt the size of S_1. The moment of the local signal histogram within a moving window is defined as

$$m = \sum_i \left(\frac{r_i}{R} \right)^2 P_i \tag{10}$$

where r_i is the ith gray level of the signal, R is the maximum value of the signal within the window, and P_i is the probability of the ith gray level within the window. From the above equation we can see that $m \in (0, 1]$.

The adaptation of l_1, the size of S_1, is based on m as described below:

$$l_1 = \lfloor (N - N_o)m \rfloor + N_o \tag{11}$$

where N is the window length and N_o is the minimum size of S_1. From Equations (10) and (11) we can see that m is large in the background region, and thus l_1 is chosen to be large. On the other hand, if the window contains defects, l_1 will be small, and consequently defects close to each other are also resolved.

The function of the structuring element S_2 in step 2 is to extract the background of the envelop signal. Therefore S_2 is fixed at value just slightly larger than the size of the defect signal. The third structuring element S_3 is used to broaden the defect features to compensate the misalignment of the defect signal in successive revolutions. This is also set to a fixed value. The structural element S_4 is of fixed size 2×1 which is determined by the check rule use in practice. The threshold s also affects POD and PFA, and is discussed in the results section.

RESULTS AND DISCUSSION

The algorithm was tested using real wheel inspection data collected at the Northwest Airlines maintenance facility. A total of 120 inspections from 45 wheels formed the experimental database. Among them 107 inspections were from good wheels and 13 inspections were from wheels with cracks. Figure 3 shows the results of applying

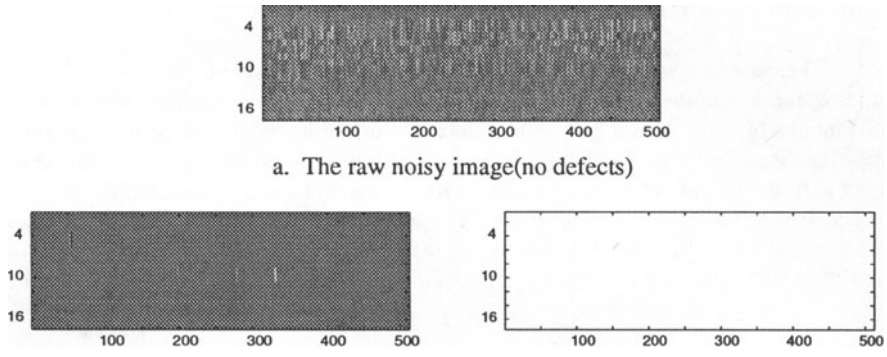

b. Filtered image using non-adaptive filter

c. Filtered image using adaptive filter(no defects)

Figure 3. Results using a noisy image from a clean wheel without defects.

the algorithm to a noisy data from a clean wheel without defects. Figure 3(a) shows the raw data; 3(b) is the filtered image using non-adaptive morphological filter which contains some indications that may be interpreted as defects, 3(c) is the filtered image using adaptive morphological filter showing no indications of defects.

The results obtained using data from a wheel with cracks are shown in Figure 4. The raw data and filtered images obtained using a non-adaptive and an adaptive filter are presented in Figures 4 (a), (b), and (c) respectively. The parameters used for the non-adaptive filter are l_1 =31, l_2=7, l_3 =3, and s =0.7. Parameters used for adaptive filter are N=512, N_o=21, l_2=7, l_3 =3, s =0.7.

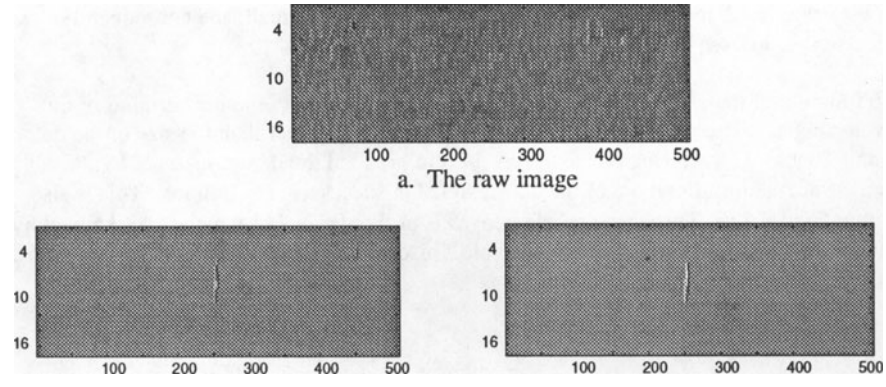

b. Filtered image using non-adaptive filter.

c. Filtered image using adaptive filter

Figure 4. Results obtained using an image from a cracked wheel.

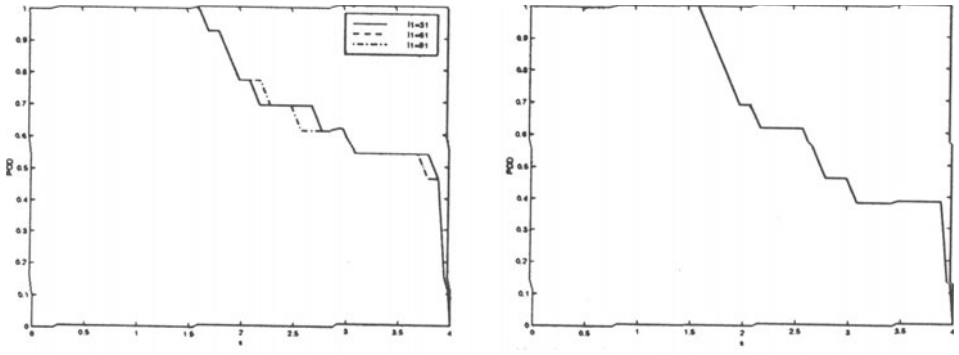

a. Non-adaptive filter. b. Adaptive filter

Figure 5. The effect of threshold s on PFA for non-adaptive and adaptive filters.

The effect of the threshold s on the POD and PFA of the non-adaptive and adaptive filter is shown in Figures 5 and 6. The adaptive scheme is seen to offer a more optimal performance of the filter. In both the non-adaptive and adaptive algorithms, the choice of threshold s is very important. Based on the experiments conducted in this study, the optimal value of s that gives the lowest PFA and at the same time keeps the highest POD is chosen to be 1.5.

For future work a mathematical model for the noise and defect signal will be developed. Such a model will be useful for conducting an analytical study of the algorithm.

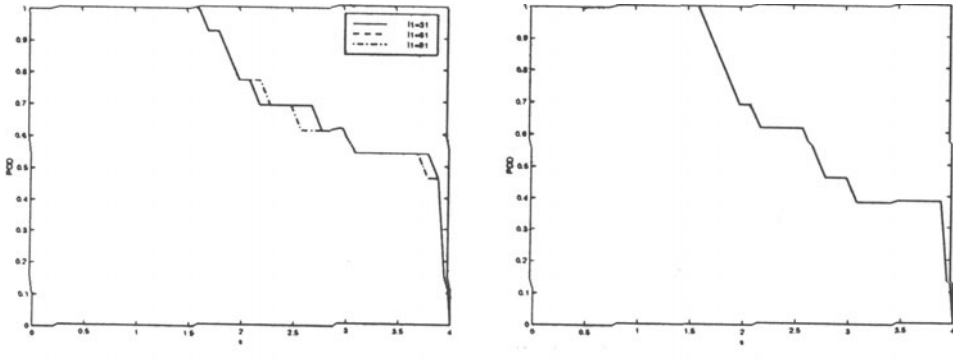

a. Non-adaptive filter. b. Adaptive filter

Figure 6. Effect of s on POD for non-adaptive and adaptive filters.

ACKNOWLEDGEMENTS

This work is supported by FAA Center for Aviation System Reliability. The help provided by Northwest Airlines in the collection of wheel inspection data at their maintenance facility is also acknowledged.

REFERENCES

1. J. Serra, *Image analysis and mathematical morphology* (Academic Press, London, 1982).
2. S. R. Sternberg, "Grayscale morphology," *Comput. Vision, Graphics, Image Processing*, vol.35, pp.333-355, 1986.
3. R. A. Peters, "A new algorithm for image noise reduction using mathematical morphology," *IEEE Trans. Image Processing*, vol. 4, no. 5, pp. 554-567, 1995.
4. D. Zhao, "Adaptive thresholding through morphological filtering," *SPIE Proc. Nonlinear Image Processing IV*, vol. 1902, pp. 148-158, 1993